Bulletin of Engineering Geology and the Environment (2019) 78:2081–2092
https://doi.org/10.1007/s10064-018-1233-6

CASE HISTORY

Dynamical process of the Hongshiyan landslide induced by the 2014 Ludian earthquake and stability evaluation of the back scarp of the remnant slope

Hai-Bo Li[1] · Xiao-Wen Li[2] · Yu Ning[3] · Shu-Fang Jiang[4] · Jia-Wen Zhou[1]

Received: 29 October 2017 / Accepted: 18 January 2018 / Published online: 1 February 2018

Abstract

Reinforcing a landslide dam and converting a landslide-dammed lake to a hydraulically engineered lake is a sound means to address this natural disaster. The Hongshiyan landslide-dammed lake reconstruction project provides an excellent example. However, the stability of the remnant slope is crucial to the reconstruction of this project. It is essential to analyse the formation failure mechanisms of the Hongshiyan landslide and evaluate the stability of the remnant slope. Combined with field investigations and unmanned aerial vehicle (UAV) 3D image technologies, the failure mechanisms of the Hongshiyan landslide and the stability of the remnant slope were qualitatively studied and discussed. The dynamic process and failure mechanism of the Hongshiyan landslide are significantly different to conventional landslides. The dynamic process of the Hongshiyan landslide can be divided into three stages: time-dependent deformation stage, earthquake-induced failure stage and an unloading recovery stage. The failure mechanism can be summarised as follows: tension–crush–shattering–sliding. The stability conditions of the remnant slope are worse than those of conventional landslides under the same conditions. Toppling and small collapse are possibly occurring at the back scarp of the remnant slope because of the steep slope gradient, well-developed tension fractures and frequent occurrence of aftershocks and rainstorms. Based on the density, opening degree, porosity and connectivity of the cracks, as well as instability risk probabilities, the rock mass of the back scarp of the remnant slope can be divided into three zones: the seismically damaged zone, the unloading damaged zone and the stable zone. To guarantee the safety of the remnant slope and reduce secondary earthquake or rainstorm disasters, corresponding comprehensive treatment measures must be taken to ensure long-term stability.

Keywords Earthquake-induced landslide · Dynamic process · Failure mechanism · Remnant slope stability · Corresponding treatments

Introduction

An earthquake-induced landslide is a common type of geo-hazard worldwide. In a mountainous area, the large scale and fast speed of earthquake-induced landslides can destroy villages, kill people, damage roads and block rivers, leading to heavy casualties and huge economic losses (Dunning et al. 2007; Ehteshami-Moinabadi and Nasiri 2017). Landslide dams pose a great threat to people and properties in both upstream areas by inundation and downstream areas by dam-breaching floods (Zhang et al. 2015; Shi et al. 2017). Converting a landslide-dammed lake to an object beneficial

✉ Jia-Wen Zhou
jwzhou@scu.edu.cn

[1] State Key Laboratory of Hydraulics and Mountain River Engineering, Sichuan University, Chengdu 610065, China

[2] College of Water Resource and Hydropower, Sichuan University, Chengdu 610065, China

[3] Power China Kunming Engineering Corporation Limited, Kunming 650051, China

[4] Sinohydro Bureau 7 Co., Ltd., Power Construction Corporation of China, Chengdu 610081, China

to mankind such as a scenic spot or hydraulically engineered area is a good means to address this natural disaster. However, ensuring the stability of the earthquake-induced rock slope and preventing secondary disasters of earthquakes are crucial to the reconstruction of the project. It is essential to analyse the formation failure mechanisms of earthquake-induced landslides and evaluate the stability of the remnant back scarps.

In recent years, earthquake-induced landslides have received increasing attention from researchers in several fields, including their spatial distribution, type and characteristics, dynamic process and formation failure mechanism (Zhou et al. 2015; Sun et al. 2017). According to the statistical analysis of 11,000 landslides induced by the 1994 Northridge earthquake (Mw 6.7), the most common types of landslides were highly disrupted shallow falls and slides of rock or debris (Harp and Jibson 1996). Keefer (1984) established a classification system that categorises earthquake-induced landslides into rock falls, rock slides, rock avalanches, rock slumps and rock block slides. Kramer (1996) summarised the failure mechanism of the earthquake-induced landslide into two types: inertial instability and weakening instability. These concepts had been applied by Biondi et al. (2002) and Bandini et al. (2015) to slope displacement analysis, and desirable effects were achieved. Xu and Dong (2011) and Huang et al. (2011) generalised the speed collapse and large deformation failure mechanism of the earthquake-induced landslide as tension–shear–sliding by field investigations of more than 20 large landslides from the 2008 Wenchuan Earthquake (Mw 8.0).

Other researchers have focused on hazard assessment, stability evaluation and landslide mitigation of earthquake-affected areas. Kobayashi et al. (1990) simulated rock falls triggered by earthquakes. Ambraseys and Srbulov (1995) examined the estimation of permanent slope displacements induced by earthquakes and presented predictive formulae and graphs for co-seismic and post-seismic permanent displacements of translational movements. Guan (2009) investigated the damage to the Zipingpu water control project induced by the Wenchuan earthquake on 12 May 2008 and evaluated its safety. Li and He (2009) analysed the instabilities and corresponding treatments of a seismically induced road slope in the region hit by the Wenchuan earthquake. Wu et al. (2010) studied the failure mechanisms of post-earthquake bedrock landslides in response to rainfall infiltration.

The Hongshiyan reconstruction project is one of the first excellent examples of addressing natural disasters by transforming the landslide-dammed lake into a hydraulically engineered lake in China (Lv et al. 2017). The stability of the earthquake-induced rock slope is crucial to the reconstruction of the project. The rock mass is highly damaged and broken, and rock fall instability phenomena at the top remnant of the back scarp pose a significant threat to construction workers and mechanical equipment at the base of the slope. It is essential to analyse the formation failure mechanisms of the Hongshiyan landslide and evaluate the stability of the remnant back scarp. Combined with field investigations, monitoring data and unmanned aerial vehicle (UAV) 3D image technologies, the dynamic process and formation failure mechanisms of the Hongshiyan landslide have been analysed, and the qualitative stability evaluation of the remnant back scarp has been studied and discussed. Finally, in order to guarantee the safety of the high rock slope and reduce secondary earthquake or rainstorm disasters, corresponding comprehensive treatment measures have been suggested to ensure the long-term stability of the remnant back scarp.

Background

Overview

On 3 August 2014, an Ms 6.5 earthquake shocked Ludian County, Yunnan Province in Southwestern China (27.1° N, 103.3° E). It resulted in 617 deaths and more than 3000 people were injured. It destroyed a significant number of houses and induced hundreds of landslides of various types, dominated by shallow slides, deep-seated slides, rock falls, debris avalanches and unstable slopes. As shown in Fig. 1a, the Hongshiyan landslide is the largest scale landslide induced by the 2014 Ludian Ms 6.5 earthquake, located on a bank of the Niulan River in Ludian County. The ensuing accumulation of mass waste blocked the river channel and formed the Hongshiyan landslide dam, with a volume of approximately 12 million m^3.

It is very difficult and expensive to excavate and dredge a landslide dam, for there is insufficient space for rock fill materials in a narrow valley. An alternative processing method is being implemented to reinforce and change it into a permanent dam (Liu 2015). The stability of the earthquake-induced rock slope is crucial to the reconstruction of the project. It is essential to analyse the formation failure mechanisms of the Hongshiyan landslide and evaluate the stability of the remnant back scarp. As shown in Fig. 1b, the Hongshiyan landslide is a typical earthquake-induced failure, and the topography and failure formation mechanisms are significantly different from the conventional landslides. Secondary earthquake or rainstorm disasters, such as toppling and small collapse at the top of the remnant back scarp, pose a significant threat to construction workers and mechanical equipment at the base of the slope.

Geological conditions

The Hongshiyan landslide is in the generating fault zone (Baogunao–Xiaohe Fault) and is only approximately 15 km away from the epicentre (Fig. 1a). In this area, the land surface is deeply incised, neotectonic movement is common, and

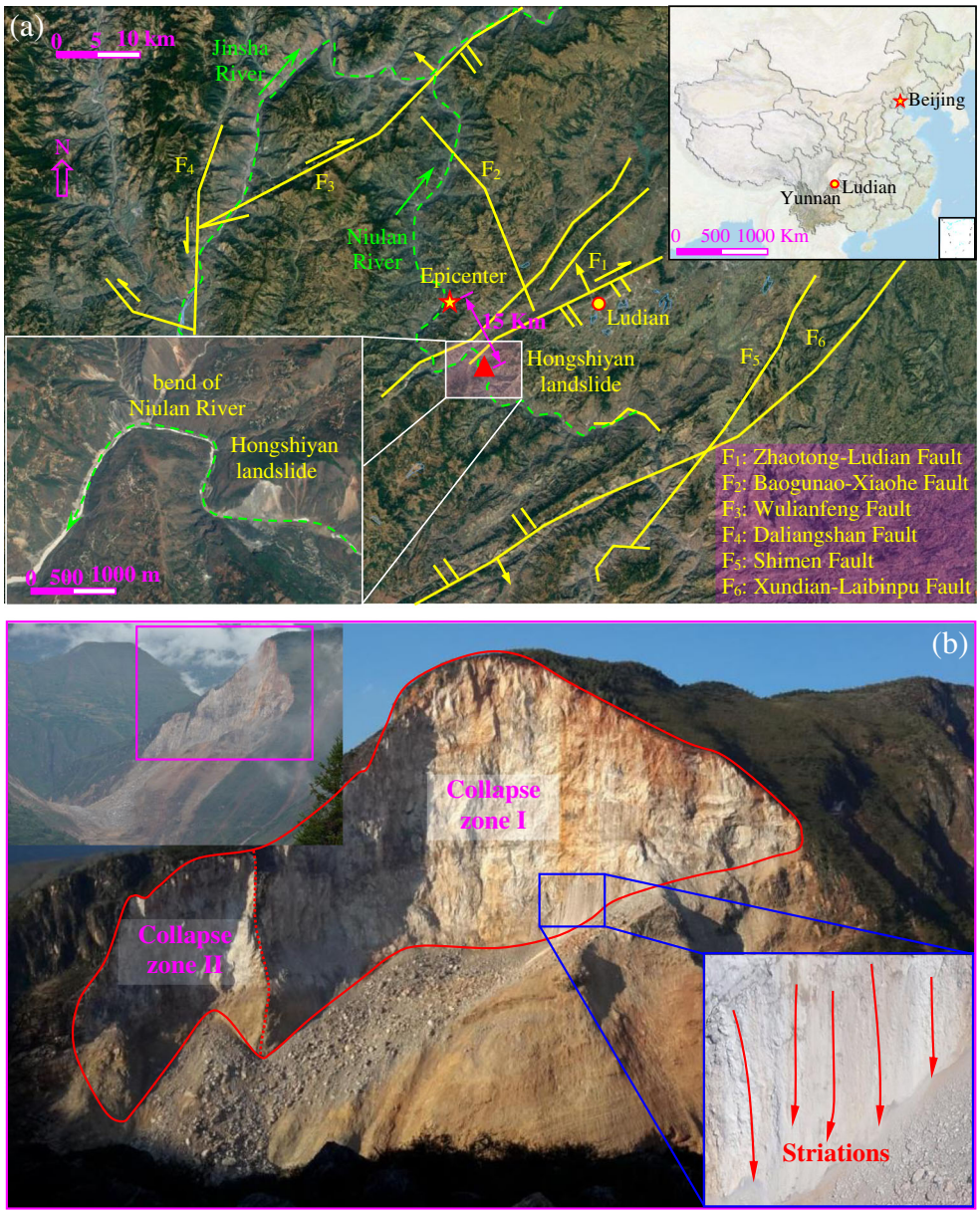

Fig. 1 Location and shape of the Hongshiyan landslide: **a** map of Hongshiyan landslide; **b** site photos of Hongshiyan landslide

strata and geological structures are complex. The development of regional faults, such as the Zhaotong–Ludian Fault (F1), Baogunao–Xiaohe Fault (F2), Wulianfeng Fault (F3) and Daliangshan Fault (F4), has a significant effect on the stability of the Hongshiyan landslide.

As shown in Fig. 2, the original Hongshiyan Mountain is exposed, with little vegetation on the surface, presenting a typical layered structure. The main strata from top to bottom are from the Permian (P), the Devonian (D) and the Ordovician (O), respectively. The rock strata mainly dip toward the mountain and its downstream side, with a strike of N20°–60°E, a dip direction to the NW and a dip angle of 10–30°. The rock masses are mainly thick or very thick limestone and dolomitic limestone at the upper part of the slope, and a thin layer of sandstone and shale at the lower part of the slope. The slope has upper-hard-and-lower-soft structural characteristics.

As a result of long-term geological movement, the rock strata present low-angled folds or flexural deformations. A fault, F_5, is developed in the middle of the slope with strike of N5°–15°W, a dip direction to the SW and a dip angle of 40–50°. F_5 is a control fault extending approximately along the whole landslide with a fault zone of typically approximately 0.5–1.0 m in thickness, and it mainly consists of fragmented rocks and fault gouges. Numerous approximately vertical structural joints and bedding joints are developed and multiply interlaced at the surface of the rock slope. The rock mass was broken, and many small cliffs can be found at the slope as a result of previous small collapses.

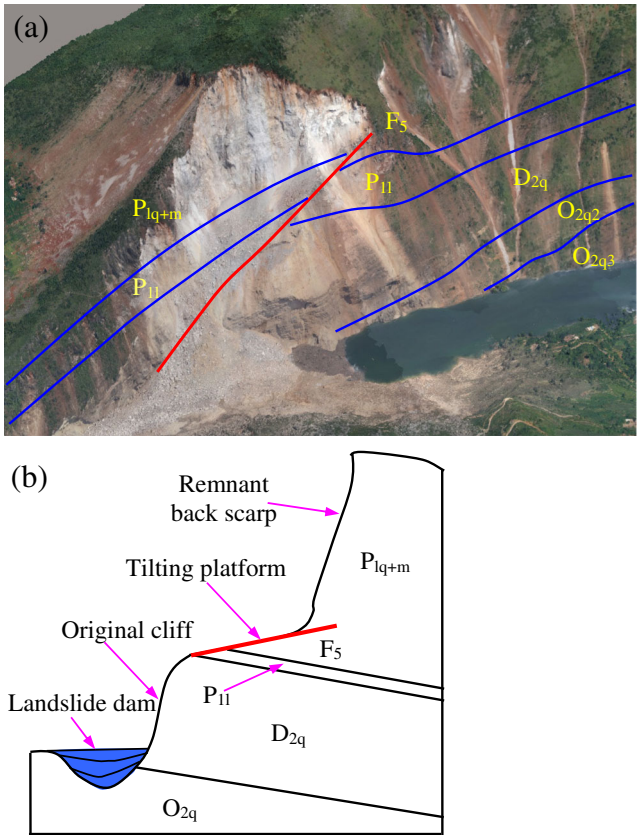

Fig. 2 Geological conditions of the Hongshiyan landslide: **a** geology of Hongshiyan landslide; **b** geologic section of Hongshiyan landslide

Topography of the Hongshiyan slope

The Hongshiyan landslide is in a narrow valley that is deeply incised. The Niulan River flows in the valley from southeast to northwest and has a width of approximately 100 m. The original Hongshiyan Mountain was located at a bend in the Niulan River and had a steep slope of 54–61° before the earthquake. It is a three-sided mountain with a height that rises approximately 760 m above the riverbed (Fig. 1a, b).

To investigate the topographical changes after the landslide, UAV technologies have been used to obtain a high-resolution 3D image model of the Hongshiyan landslide. As shown in Fig. 3, after the 2014 Ludian Ms 6.5 earthquake, the topography of Hongshiyan Mountain changed significantly. The aspect of the Hongshiyan landslide presents a huge chair shape. A tilting platform with the strata gently dipping toward the mountain and the downstream side divide the slope into two parts; the upper part of the slope is a huge remnant back scarp with a height of 350 m and a total width of approximately 900 m along the river; the lower part is an original cliff with a height of 120 m. The back edge of the landslide is large, steep and rough, and it forms the main failure surface. In contrast, the shear sliding surface at the forward edge of the landslide is short and smooth, with obvious striations. Two connected collapse zones (I and II) can be obviously distinguished from the landslide surface.

Approximately 12 million m^3 of rock slid into the Niulan River to form a huge V-shaped landslide dam. The formed landslide-dammed lake is estimated to have a catchment area of 11,800 km^2, a lake capacity of 2.6×10^8 m^3 and a maximum length of the backwater area of 25 km. There are favourable conditions and unique advantages of converting the Hongshiyan landslide-dammed lake into a hydraulically engineered lake.

Formation mechanism of the Hongshiyan landslide

Mass movement process

The Hongshiyan landslide is a typical earthquake-induced failure. The unique terrain and the seismic loads are the main reasons for the landslide. As shown in Fig. 4a, under the instantaneous seismic loadings of the 2014 Ludian Ms 6.5 earthquake, tension fractures extended and transfixed rapidly, which formed the steeply sloped open surface of the back edge. At the same time, shear failure suddenly occurred along weak structural planes near the fault zone of F_5 and formed the sliding surface of the forward edge. The slope in collapse zone I failed and slid toward the free surface. Folding and collapse occurred because of the steeply sloped open surface of the back edge. Rock masses fell, hit the bulgy tilting platform and broke into pieces. The weathered and relatively broken anti-sliding rock body at the tilting platform then suddenly collapsed and was crushed. The landslide preferentially developed in this direction and made it the main sliding bed. The sudden crushing of the anti-sliding rock body and the scarps of the main sliding bed in turn induced collapse II (Figs. 1b and 4a). Part of the landslide body slid over the up-inclined tilting platform and left multiple striations and scratches, making it an obvious scarping zone.

Approximately 12 million m^3 of rock collapsed from the upper part of Hongshiyan Mountain, hit and scarped the tilting platform, crushed and slid into the Niulan River to form a huge V-shaped landslide dam. Combined with UAV 3D image modelling technology and field sampling, the particle size distribution of the landslide dam has been studied. As shown in Fig. 4a, b, the avalanche masses are generally small; the biggest particle size of rock mass is less than 20 m and huge stones (having a particle size that exceeds 2 m) account for just 10% of the mass.

Failure mechanism

As shown in Figs. 1b and 4a, the Hongshiyan landslide is basically controlled by topographic conditions and strong

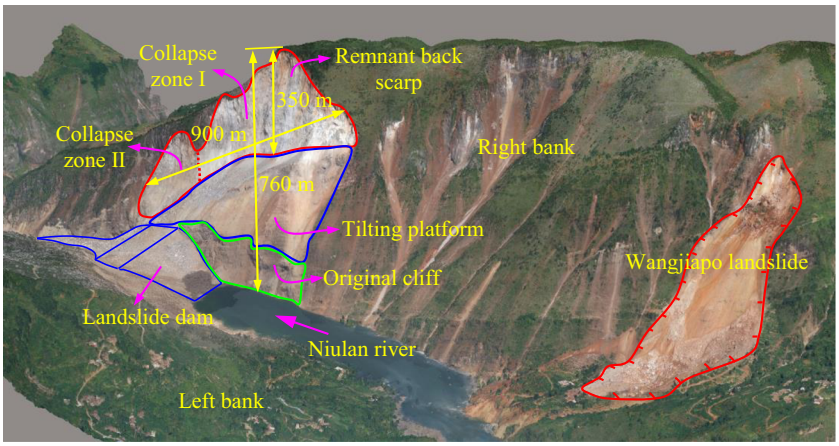

Fig. 3 High-resolution 3D image model of the Hongshiyan landslide

seismic dynamic failure. The dynamic process of the Hongshiyan landslide can be divided into three stages: a time-dependent deformation stage, an earthquake-induced failure stage and an unloading recovery stage.

As shown in Fig. 5a, in its virgin state, and due to long-term weathering and gravity effects, the original slope is gradually deforming toward the free surface because of the upper-hard-and-lower-soft structural characteristics and development of

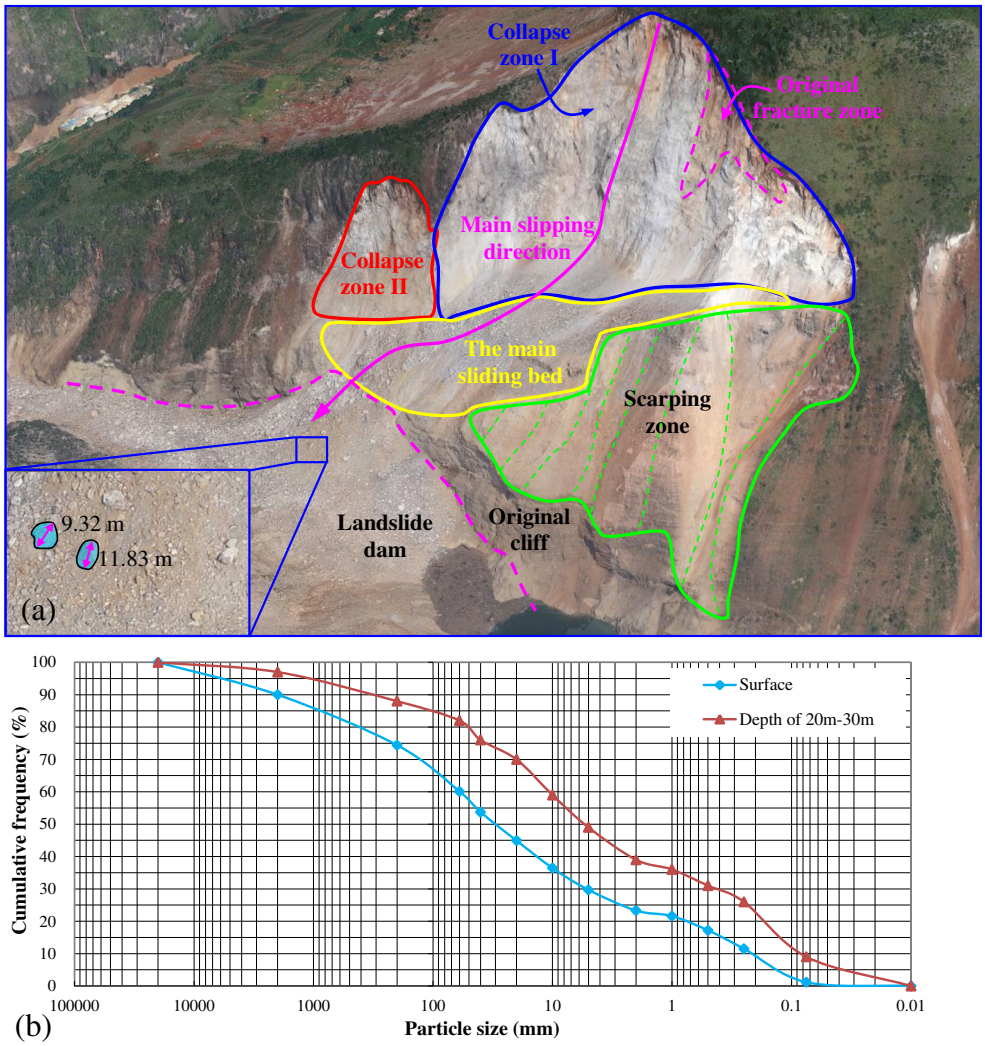

Fig. 4 Field investigation of the Hongshiyan landslide: **a** dynamic process of the earthquake-induced Hongshiyan landslide; **b** particle size distribution of the landslide dam

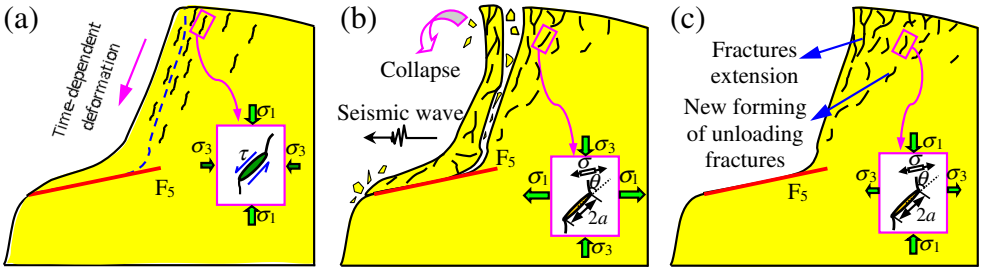

Fig. 5 Failure mechanism of the Hongshiyan landslide: **a** time-dependent deformation stage; **b** earthquake-induced failure stage; **c** unloading recovering stage

the controlling fault F_5. Tension stresses are concentrated at the upper edge of the slope. As a consequence, micro-crack initiation, propagation and coalescence occur and finally develop into many controlling fractures approximately parallel to the free surface. For example, a marked original fracture, which is eroded probably by aperture and water circulation, can be observed at the top edge of the slope (Fig. 4a). These fractures are recognised as the plane along which the collapse occurred. The tension fractures and fault F_5 cut the slope, making it a potentially unstable block.

During the sudden strong earthquake, the seismic waves had a complex effect on Hongshiyan Mountain. The seismic waves continued for approximately 30 s, and the peak earthquake acceleration reached more than 9.00 $m.s^{-2}$. The seismic accelerations in the horizontal direction (peak of 9.34 $m.s^{-2}$) were much greater than those in the vertical direction (peak of 4.33 $m.s^{-2}$) (Liu et al. 2016; Hong et al. 2016). The Hongshiyan landslide is located at the southernmost termination of the Ludian primary earthquake surface rupture zone, and the seismic intensity reached VIII. The left-lateral motion of the southwestern wall of the Baogunao–Xiaohe Fault (F_2) has a remarkable influence in the occurrence of the Hongshiyan landslide (Xu et al. 2015). The adverse terrain and geological conditions and the steep bulge shapes (three-sided hanging) had a significant seismic amplification effect on Hongshiyan Mountain (Pedersen et al. 1994; Ashford and Sitar 1997; Sepúlveda et al. 2005; Bouckovalas and Papadimitriou 2005; Rizzitano et al. 2014). As shown in Fig. 5b, under the instantaneous seismic loadings of the 2014 Ludian Ms 6.5 earthquake, the slope is in a tension–compression cycle stress state induced by the horizontal acceleration seismic waves. Tension stress significantly concentrates at the tips of the pre-existing cracks and massive tension cracks extend, transfixing and forming the steeply sloped open surface of the back edge. Then, tension–shear failure occurs in the weak zone of the controlling fault F_5 and forms the steep column-shaped sliding block. The seismic waves have a complex propagation in the unstable sliding block, particularly between the discontinuity interfaces. The rock mass under the complex tension–compression cycle stress is broken and crushed into pieces, shattering and collapsing suddenly. The crushed rock masses "pour down" similar to avalanches. This can be verified, as the striations can only be found at the forward edge and at the bottom of the back edge of the landslide (as shown in Fig. 1b), and the particle size of the avalanche masses is generally small (as shown in Fig. 4b).

As shown in Fig. 5c, once the landslide occurs, tension stress relieves instantaneously. The rock mass is in an instantaneous unstable stress state, and its rebound deforms toward the mountain side instantly. The sudden unloading and rebounding leads to tension stress concentrated at the tips of the pre-existing fractures (Cai 2008; Li et al. 2017). The fractures extend rapidly, and the rock mass at the back scarp of the remnant slope is highly damaged. Stress redistributes and spreads into the deeper rock mass of the slope and gradually reaches a new balance. This, in turn, induces the initiation, propagation and coalescence of new cracks, and new unloading damage occurs at the back scarp of the remnant slope. Toppling and small collapse tend to occur during this stage.

The seismic loads and the steep terrain are the main reasons for the formation of the Hongshiyan landslide. The seismic waves have a complex propagation and effect on the rock mass, particularly for the discontinuities in the slope, which induces damage and large steep tension fractures forming the back edge of the landslide. The slope is totally cut off by the large steep tension fracture and controlling fault F_5. At the same time, the unstable rock block is damaged and crushed under the complex tension–compression cycle stress state. Shattering and sliding occurs suddenly along the formed surfaces. The formation failure mechanism of the Hongshiyan landslide can be summarised as tension–crush–shattering–sliding.

Stability analysis of the remnant slope

Current status analysis of the remnant slope

There are favourable conditions and unique advantages of the Hongshiyan landslide-dammed lake for conversion into a hydraulically engineered lake. However, the stability of the remnant slope is crucial to the reconstruction of the project. As shown in Figs. 1b and 4a, the remnant slope has a step-like shape, a tilting platform with the strata gently dipping toward the mountain and the downstream side dividing the slope into two parts; the upper part of the slope is a steep cliff induced by the Hongshiyan landslide with a height of 350 m, and its rock

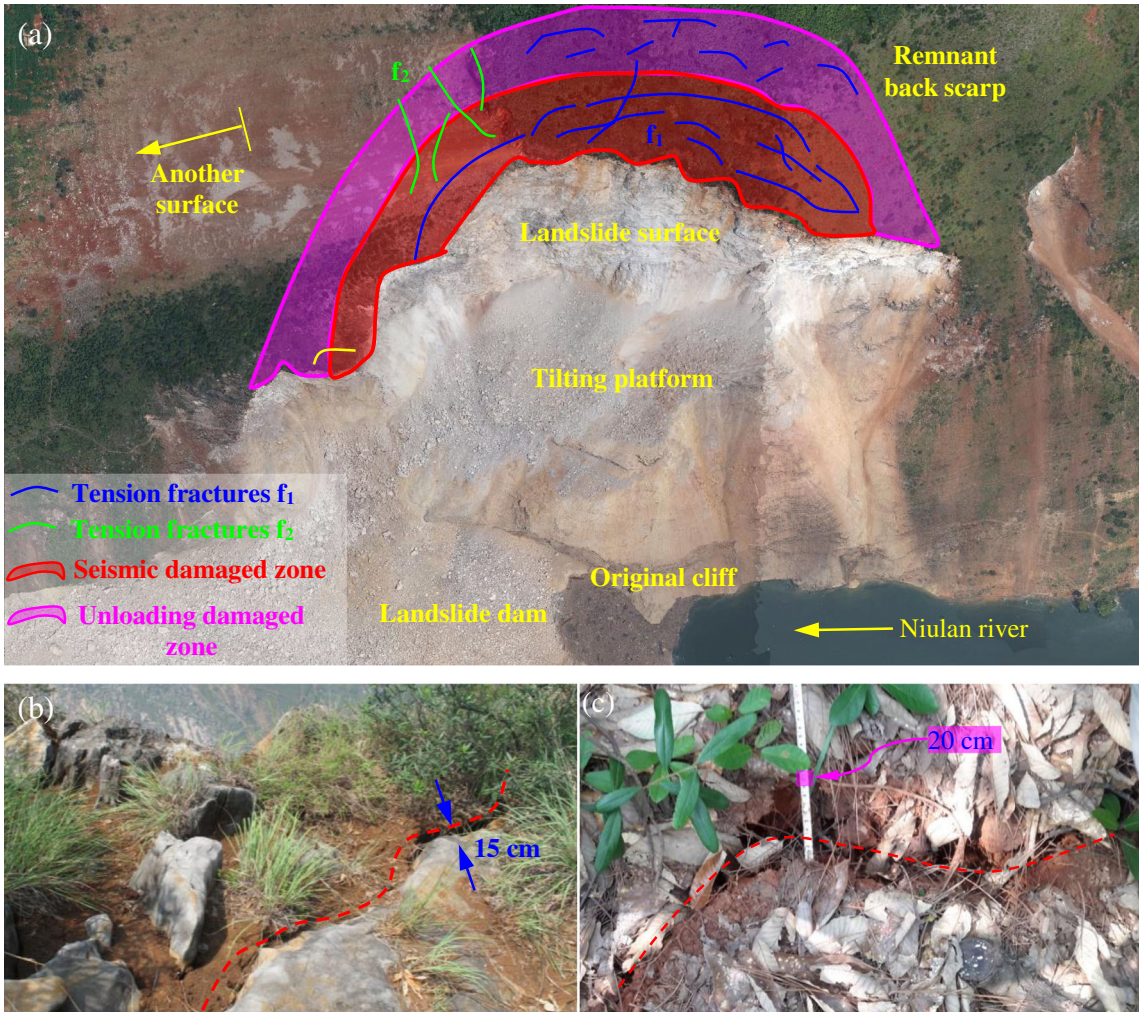

Fig. 6 Tension fracture and damage zone distribution on the remnant slope: **a** damage zone distribution on the remnant slope; **b** tension fracture zigzagging downstream of the top edge of the remnant slope; **c** tension fractures in the unloading damaged zone

masses are mainly thick or very thick fresh limestone and dolomitic limestone; the lower part is an original cliff that consists of a thin layer of sandstone and shale. The rock strata mainly dip toward the mountain and downstream side, which is favourable for the stability of the rock slope.

There is no regional large fault passing through the remnant slope area. Only a moderate fault F_5 developed in the middle of the slope. However, the major rock mass has collapsed, and there is no obvious potentially unstable rock block. The slope is stable overall, while toppling and small collapse along the edge of the back scarp of the remnant slope should be a focus of future reinforcement and later operation of the project, particularly at the area near the top edge of the slope.

Damage analysis of the back scarp of the remnant slope

The rock mass at the back scarp of the remnant slope is highly damaged not only from the seismic loadings during the earthquake but also from the unloading damage during the time-dependent deformation stage and the unloading recovering stage after the earthquake. Numerous tension and unloading cracks are developed in the back scarp of the remnant slope. To evaluate the stability of the remnant slope, UAV 3D image technology was used to identify fractures and investigate geological conditions. As shown in Figs. 6 and 7, based on the high-resolution 3D image model of the remnant slope and field geological investigations, the distribution and occurrence features of the fractures have been analysed, as shown in Fig. 7b. The results show that there are two groups of preferred fractures which developed in the top area of the back scarp of the remnant slope.

One group of the preferred fractures f_1 is mainly distributed in nearly east-west directions with steep dip angles of 78–83°. The majority of the cracks are open, and one of the widest cracks found in this area reaches 30–40 cm in width, with a visible depth of 1.0–1.5 m and stretching for 3–15 m. The longest crack reaching 60 m is found at a distance of 12–

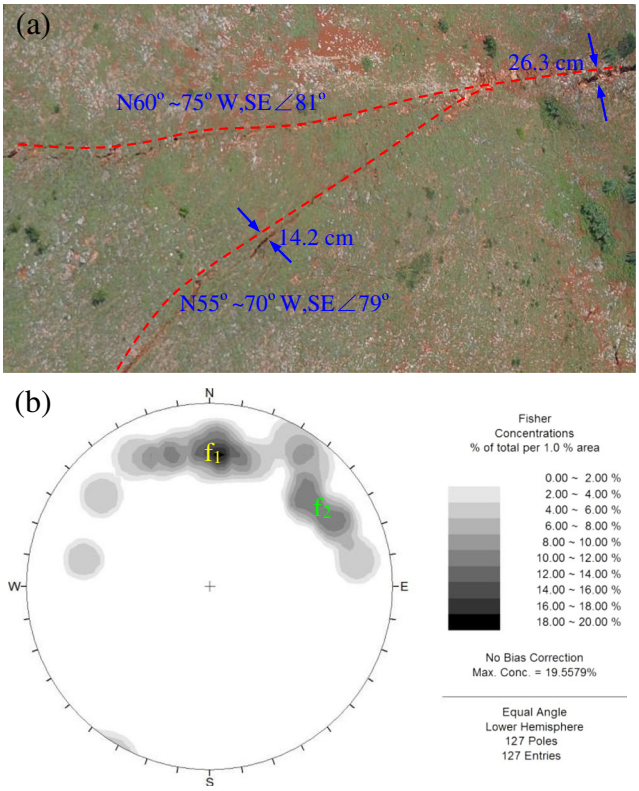

Fig. 7 Fracture identification and statistics using unmanned aerial vehicle (UAV) 3D image technology: **a** fracture identification; **b** fracture statistics

20 m from the top edge of the slope with an open width of 10–15 cm and a visible depth of 1.0–1.5 m, zigzagging to the downstream side of the top edge of the slope (Fig. 6b). The other cracks are distributed in various sizes, and most of them stretch approximately parallel to the landslide surface, followed by some stretching approximately perpendicular to the surface.

Another group of preferred fractures f_2 is developed at the downstream top area of the slope, approximately perpendicular to the landslide surface because of unloading failure in another steep free surface downstream of the slope. The fractures f_2 are approximately parallel to the downstream free surface of the slope with a strike of N15°–55°E, a dip direction to the NW and a dip angle of 76–83°. However, the stretch lengths, opening widths and visible depths of the fractures f_2 are much lower than those of the fractures f_1. Another notable feature is that the density, opening degree, porosity and connectivity of the fractures, whether f_1 or f_2, decrease with distance from the edge of the slope, as shown in Fig. 6a.

These tension fractures, combined with original disadvantaged structural surfaces, such as interlaminar shear cracks and structural joints, form the main discontinuities at the back scarp of the remnant slope. The rock mass is highly damaged and broken, and the rock fall instability phenomena at the back scarp of the remnant slope pose a significant threat to the construction workers and mechanical equipment at the base of the slope.

Toppling and collapse analyses of the remnant slope

The stability problem of the rock mass at the back scarp of the remnant slope is prominent under unfavourable conditions, such as aftershocks and rainstorms, because the tension cracks, new unloading cracks, original disadvantage structure surfaces and block bodies combine under these factors.

As shown in Fig. 8a, aftershocks have occurred frequently in the Hongshiyan landslide area since the 2014 Ludian Ms 6.5 earthquake. By the end of August 2017, at least 32 aftershocks registering a 3.0 magnitude or higher have followed the main temblor. These aftershocks have a great effect on the security and stability of slopes, especially for earthquake-induced slopes such as the remnant slope of the Hongshiyan landslide. As shown in Fig. 9a, the aftershocks have a similar effect mechanism as that of the main tremblor on the slopes. The bulge shape (three-sided hanging) and the steep slope surface have a significant seismic amplification effect on the back scarp of the remnant slope. Moreover, the deep steep tension fractures cut the rock mass at the back scarp of the remnant slope into many column-shaped potentially unstable rock blocks, which means that the relatively independent potentially unstable blocks were more strongly affected by seismic loadings during the aftershock. At the same time, a wedge-splitting effect should not be ignored as seismic loading provides a tension–compression cycle stress state during the aftershock. In the compression stress state, the tension fractures have a closing tendency, while the existence of debris falling during the previous formation and expansion of tension fractures would cause splitting stresses at the tips of the tension fractures (Feng et al. 2009; Zhou et al. 2013). As the seismic accelerations generally decrease from the top to the bottom of the slope, the differential distribution of seismic acceleration would induce shear stress concentrations at the tips of the tension fractures. As a consequence, the tension fractures have a tendency to propagate along the shear stress and toward the landslide surface. Finally, tension–shear failure occurs, and toppling and small collapses occur (Zhou et al. 2010; Stead and Wolter 2015).

As shown in Fig. 8b, the Hongshiyan landslide area in southwestern China belongs to a typical mainland monsoon climate; rainfall occurs unevenly throughout the year, mainly from July to September. The annual average precipitation is 852.8 mm, while the precipitation from July to September reaches 579.9 mm, accounting for approximately two-thirds of the annual precipitation. The maximum monthly precipitation even reaches 326.0 mm. As shown in Fig. 9b, heavy rainfall has a notable effect on the security and stability of the remnant slope. Rainfall infiltration forms a hydrostatic pressure zone on the back edge of the tension fracture and

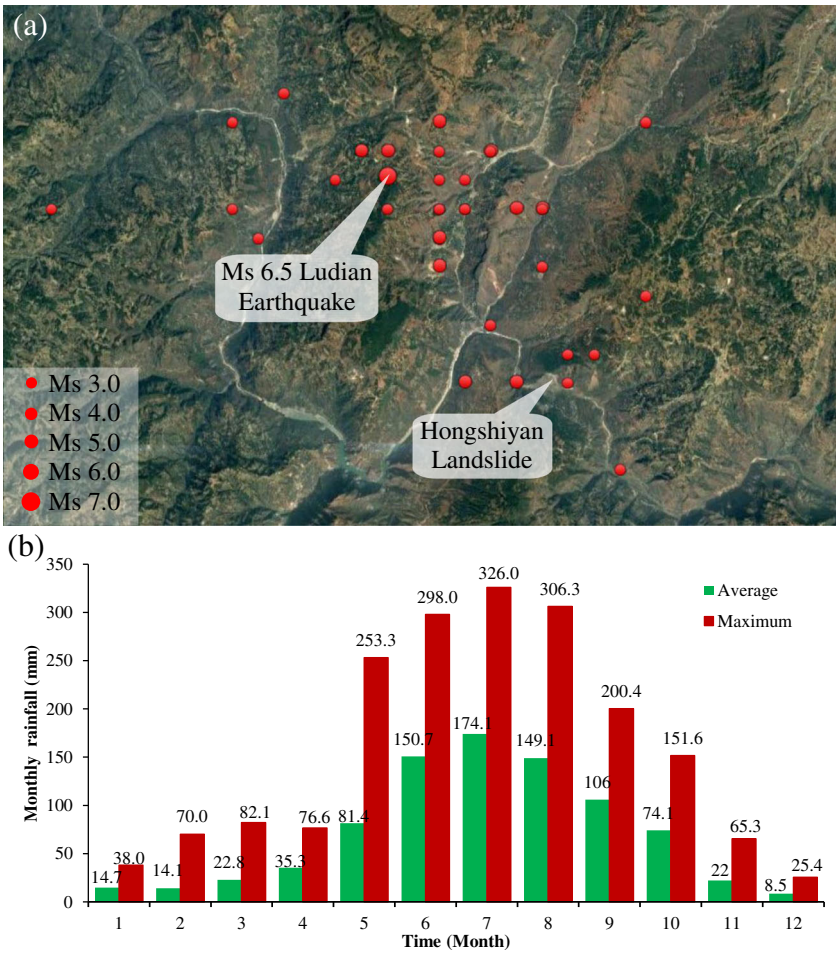

Fig. 8 Unfavourable conditions at the Hongshiyan landslide area: **a** aftershock occurrence at the Hongshiyan landslide area since the 2014 Ludian Ms 6.5 earthquake; **b** monthly average rainfall in Ludian County

induces new extension of the tension fractures. Due to the existence of the potential shear surface, which dips toward the landslide surface, hydrodynamic pressure is induced by persistent rainfall infiltration, affecting and eroding the potential shear surface. At the same time, rapid rainfall infiltration forms an uplift pressure, increases the pore water pressure and reduces the effective stress of the rock block. Moreover, rainfall infiltration has a significant softening effect, which softens the rock mass and the structural plane and reduces the effective cohesion and internal friction angle. In summary, persistent rainfall infiltration not only softens rock mass and reduces rock mass mechanical indicators, but it also composes the main load on the rock block. Toppling and small collapse are caused by the softening of the rock mass, erosion of the potential shear surface, reduction of effective stress and the corresponding stress adjustment of the rock slope due to rapid rainfall infiltration (Alejano et al. 2010; Smith 2015).

In an extreme circumstance where an aftershock occurs during the rainy season, under the tension–compression cycle stress state, the tension fracture and shear surface have an instantaneous closing tendency because of the compression stress, the pore space volume decrease and pore water passage blockage. The pore water cannot be dissipated promptly, inducing an instant excessive static pore water pressure and decreasing the effective stress. Tension fractures extend rapidly because of the coupling effect of tension and shear stress, as well as the excess static pore water pressure accumulation. This mechanism is similar to the wedge-splitting effect, which would induce rapid toppling and collapse at the back scarp of the remnant slope.

Therefore, the remnant slope is stable overall, while toppling and small collapse are possibly occurring along the edge of the landslide surface, particularly at the back scarp of the remnant slope because of the steep landslide surface, well-developed tension fractures, highly damaged rock mass and frequent occurrence of aftershocks and rainstorms.

Discussions

Specialty of Hongshiyan landside

The Hongshiyan landslide is a typical earthquake-induced failure; however, the failure mode and formation mechanisms are significantly different from conventional landslides. For the conventional landslide shown in Fig. 10a, the stress at

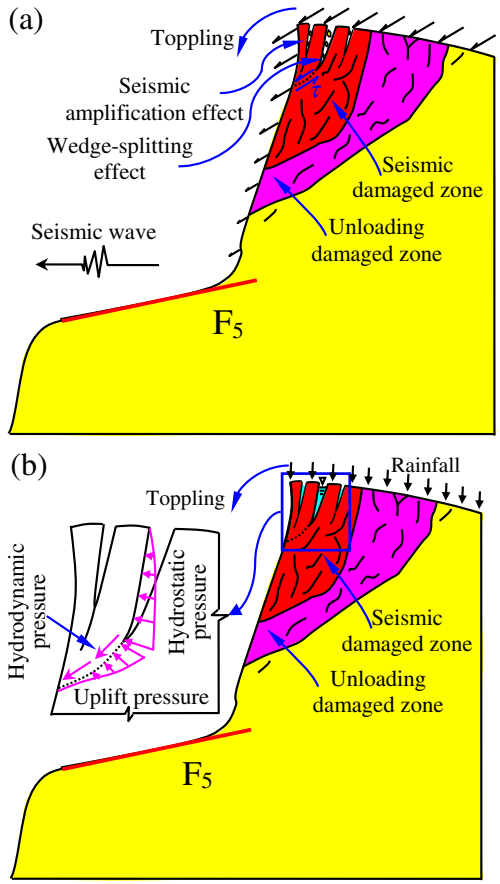

Fig. 9 Toppling and collapse analysis of the rock mass at the back scarp of the remnant slope under aftershock conditions (**a**) and under rainstorm conditions (**b**)

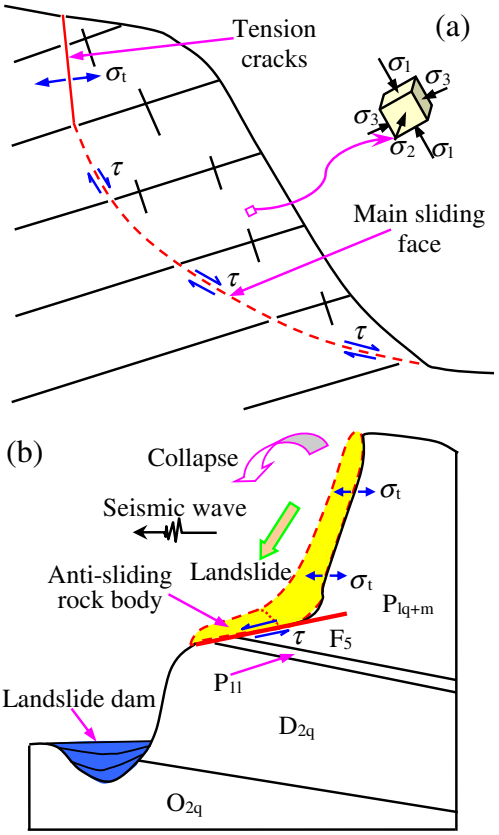

Fig. 10 Failure mechanism comparison between the Hongshiyan landslide and a conventional landslide: **a** conventional landslide; **b** Hongshiyan landslide

the surface of the slope can be summarised as the following state: the maximum principal stress σ_1 is approximately parallel to the surface of the slope, the minimum principal stress σ_3 is approximately perpendicular to the surface of the slope and the intermediate principal stress σ_2 is approximately parallel to the strike of the slope. The slope failure follows the principle of limit equilibrium and the Mohr–Coulomb criterion. The minimum principal stress σ_3 is a compressive stress and, at best, a small unloading tension stress. Shear stress concentrations initially occur at the weak faces and the slope toe. Then, a short shear slip belt forms and gradually pierces. The slope deforms toward the free surface, inducing tension stress concentrated at the upper edge of the slope. In addition, tension fractures finally occur and the landslide befalls (Brideau et al. 2009; Clague and Stead 2012).

For the Hongshiyan landslide shown in Fig. 10b, the seismic loads first induce numerous tension fractures, forming the steeply sloped open surface of the back edge. Then, tension–shear failure occurs along the controlling fault zone of F_5 and forms the sliding surface of the forward edge because of the continuous acceleration seismic waves. The sliding block is shattered and crushed under the complex tension–compression cycle stress. The crushed rock masses "pour down" as avalanches rather than sliding off as conventional landslides. The large steeply sloped open surface of the back edge is the main failure face that controls the Hongshiyan landslide. In addition, large numbers of tension fractures developed at the back scarp of the remnant slope of the Hongshiyan landslide. These fractures are basically steep, open and approximately parallel to the free surface (Fig. 6b, c). As for conventional landslides, the shear slip faces in the forward edge usually control the slope failure and the tension fractures at the top edge are much smaller and shallower in comparison to those of the Hongshiyan landslide.

Corresponding treatments for the remnant slope

The steep landslide surface, highly damaged rock mass and the well-developed fractures have a remarkable effect on the stability of the remnant slope. The stability condition of the remnant slope after the Hongshiyan landslide is worse than that of a conventional landslide under the same conditions. Toppling and small collapse are most likely to occur under unfavourable conditions, such as aftershocks and rainstorms.

Due to the density, opening degree, porosity and connectivity of the fractures, as well as the instability risk

probabilities of the rock mass, the remnant slope can be divided into three zones: the seismically damaged zone, the unloading damaged zone and the stable zone (as shown in Figs. 6a and 9). The seismically damaged zone is near the edge of the landslide surface with a width of 10–30 m, and the rock mass is highly damaged because of the earthquake, the sudden dynamic unloading and the rebounding deformation after the landslide. Tension fractures are densely developed with a spacing of approximately 5 m. These fractures are approximately parallel to the landslide surface with a wide opening of 1–40 cm. Toppling and small collapse are most likely to occur in this area because of the steep landslide surface, highly damaged rock mass and tension opening fractures. The unloading damaged zone is next to the seismically damaged zone and approximately 40–60 m from the edge of the landslide surface. Numerous unloading fractures developed in this area, while the density and opening degree generally do not exceed 5 m and 15 cm, respectively, which are much smaller than those of the seismically damaged zone. The rock mass is stable in a static state, while tension cracks are increasing continuously because of the time-dependent unloading and deformation induced by the steep landslide surface. Unloading failure may occur in this area if the seismically damaged zone fails and slides without treatment. Outside the unloading damaged zone is the stable zone, where few cracks can be found and the rock mass is relatively intact and stable.

Hence, in order to guarantee the safety of the high rock slope and reduce secondary earthquake or rainstorm disasters, comprehensive treatment measures must be taken to ensure the long-term stability of the remnant slope. Slope cutting must be used to clean the unstable rock mass in the seismically damaged zone and the unloading damaged zone, reducing the slope and increasing stability. Active support systems, such as rock bolts, prestressed cables and shotcrete–bolting–mesh are applied to strengthen the slope and reduce unloading damage. Coaction of rock bolts and shotcrete are employed to reinforce potentially unstable rock blocks. Closing treatment and concrete replacement are used for the unexcavated fractures and weak structural planes. Loose bodies and local potentially unstable rock masses along the edge of the remnant slope should be eliminated, and a passive prevention net must be set to prevent gravel slide. Slope protection and drainage systems must be set at the stable zone along the ridge line. Finally, much greater importance should be attached to slope stability monitoring and early warning.

Conclusions

The dynamic process and formation failure mechanism of the Hongshiyan landslide are significantly different from conventional landslides. Combined with field investigations and unmanned aerial vehicle (UAV) 3D image technology, the formation failure mechanism of the Hongshiyan landslide has been qualitatively analysed, and the stability evaluation of the remnant slope has been qualitatively studied and discussed. The following can be concluded from this study:

1. The Hongshiyan landslide is a typical earthquake-induced failure, with seismic loads and the adverse terrain being the main reasons for its formation.
2. The dynamic process and formation failure mechanisms of the Hongshiyan landslide are obviously different from conventional landslides. The dynamic process of the Hongshiyan landslide can be divided into three stages: a time-dependent deformation stage, an earthquake-induced failure stage and an unloading recovery stage. The failure mechanism can be summarised as tension–crush–shattering–sliding.
3. Toppling and small collapse are possibly occurring at the top edge of the back scarp of the remnant slope because of the steep landslide surface, well-developed tension fractures, highly damaged rock mass and the frequent occurrence of aftershocks and rainstorms.
4. To evaluate the stability and propose reasonable treatment measures, the remnant slope can be divided into three zones: the seismically damaged zone, the unloading damaged zone and the stable zone.
5. To guarantee the safety of the high rock slope and reduce secondary earthquake or rainstorm disasters, corresponding comprehensive treatment measures must be taken to ensure the long-term stability of the remnant slope.

Acknowledgements This work is supported by the National Natural Science Foundation of China (41472272) and the Youth Science and Technology Fund of Sichuan Province (2016JQ0011). Critical comments by the anonymous reviewers greatly improved the initial manuscript.

References

Alejano LR, Gómez-Márquez I, Martínez-Alegría R (2010) Analysis of a complex toppling-circular slope failure. Eng Geol 114(1):93–104

Ambraseys N, Srbulov M (1995) Earthquake induced displacements of slopes. Soil Dyn Earthq Eng 14:59–71

Ashford SA, Sitar N (1997) Analysis of topographic amplification of inclined shear waves in a steep coastal bluff. Bull Seismol Soc Am 87(3):692–700

Bandini V, Biondi G, Cascone E, Rampello S (2015) A GLE-based model for seismic displacement analysis of slopes including strength degradation and geometry rearrangement. Soil Dyn Earthq Eng 71:128–142

Biondi G, Cascone E, Maugeri M (2002) Flow and deformation failure of sandy slopes. Soil Dyn Earthq Eng 22(9):1103–1114

Bouckovalas GD, Papadimitriou AG (2005) Numerical evaluation of slope topography effects on seismic ground motion. Soil Dyn Earthq Eng 25(7):547–558

Brideau MA, Yan M, Stead D (2009) The role of tectonic damage and brittle rock fracture in the development of large rock slope failures. Geomorphology 103(1):30–49

Cai M (2008) Influence of intermediate principal stress on rock fracturing and strength near excavation boundaries—insight from numerical modeling. Int J Rock Mech Min Sci 45(5):763–772

Clague JJ, Stead D (2012) Landslides: types, mechanisms and modeling. Cambridge University Press, Cambridge

Dunning SA, Mitchell WA, Rosser NJ, Petley DN (2007) The Hattian Bala rock avalanche and associated landslides triggered by the Kashmir Earthquake of 8 October 2005. Eng Geol 93(3–4):130–144

Ehteshami-Moinabadi M, Nasiri S (2017) Geometrical and structural setting of landslide dams of the central Alborz: a link between earthquakes and landslide damming. Bull Eng Geol Environ. https://doi.org/10.1007/s10064-017-1021-8

Feng W, Xu Q, Huang R (2009) Preliminary study on mechanical mechanism of slope earthquake-induced deformation. Chin J Rock Mech Eng 28:3124–3130

Guan ZC (2009) Investigation of the 5.12 Wenchuan earthquake damages to the Zipingpu water control project and an assessment of its safety state. Sci China Ser E Technol Sci 52(4):820–834

Harp EL, Jibson RW (1996) Inventory of landslides triggered by the 1994 Northridge, California earthquake. Bull Seismol Soc Am 86(1B): S319–S332

Hong H, You J, Bi X (2016) The Ludian earthquake of 3 August 2014. Geomat Nat Haz Risk 7(2):450–457

Huang R, Xu Q, Huo J (2011) Mechanism and geo-mechanics models of landslides triggered by 5.12 Wenchuan earthquake. J Mount Sci 8(2):200–210

Keefer DK (1984) Landslides caused by earthquakes. Geol Soc Am Bull 95(4):406–421

Kobayashi Y, Harp EL, Kagawa T (1990) Simulation of rockfalls triggered by earthquakes. Rock Mech Rock Eng 23(1):1–20

Kramer SL (1996) Geotechnical earthquake engineering. Prentice Hall, Upper Saddle River, NJ

Li X, He S (2009) Seismically induced slope instabilities and the corresponding treatments: the case of a road in the Wenchuan earthquake hit region. J Mount Sci 6(1):96–100

Li HB, Liu MC, Xing WB, Shao S, Zhou JW (2017) Failure mechanisms and evolution assessment of the excavation damaged zones in a large-scale and deeply buried underground powerhouse. Rock Mech Rock Eng 50(7):1883–1900

Liu N (2015) Hongshiyan landslide dam danger removal and coordinated management. Front Eng Manage 1(3):308–317

Liu CZ, Ge YG, Jiang XY, Guo YY (2016) Dynamic analysis of the Hongshiyan collapse triggered by Ludian earthquake. J Disaster Prev Mitigation Eng 36(4):601–608

Lv Q, Liu Y, Yang Q (2017) Stability analysis of earthquake-induced rock slope based on back analysis of shear strength parameters of rock mass. Eng Geol 228:39–49

Pedersen H, Le Brun B, Hatzfeld D, Campillo M, Bard PY (1994) Ground-motion amplitude across ridges. Bull Seismol Soc Am 84(6):1786–1800

Rizzitano S, Cascone E, Biondi G (2014) Coupling of topographic and stratigraphic effects on seismic response of slopes through 2D linear and equivalent linear analyses. Soil Dyn Earthq Eng 67:66–84

Sepúlveda SA, Murphy W, Jibson RW, Petley DN (2005) Seismically induced rock slope failures resulting from topographic amplification of strong ground motions: the case of Pacoima Canyon, California. Eng Geol 80(3):336–348

Shi ZM, Xiong X, Peng M, Zhang LM, Xiong YF, Chen HX, Zhu Y (2017) Risk assessment and mitigation for the Hongshiyan landslide dam triggered by the 2014 Ludian earthquake in Yunnan, China. Landslides 14(1):269–285

Smith JV (2015) Self-stabilization of toppling and hillside creep in layered rocks. Eng Geol 196:139–149

Stead D, Wolter A (2015) A critical review of rock slope failure mechanisms: the importance of structural geology. J Struct Geol 74:1–23

Sun P, Li R, Jiang H, Igwe O, Shi J (2017) Earthquake-triggered landslides by the 1718 Tongwei earthquake in Gansu Province, northwest China. Bull Eng Geol Environ 76:1281–1295. https://doi.org/10.1007/s10064-016-0949-4

Wu Y, He SM, Li XP, Luo Y (2010) Failure mechanism and diagnosis method of dangerous crack rock after earthquake. J Sichuan Univ (Eng Sci Edition) 42(5):185–190

Xu Q, Dong XJ (2011) Genetic types of large-scale landslides induced by Wenchuan earthquake. Earth Sci J China Univer Geosci 36(6): 1134–1142

Xu X, Xu C, Yu G, Wu X, Li X, Zhang J (2015) Primary surface ruptures of the Ludian Mw 6.2 earthquake, southeastern Tibetan plateau, China. Seismol Res Lett 86(6):1622–1635

Zhang S, Xie X, Wei F, Chernomorets S, Petrakov D, Pavlova I, Tellez RD (2015) A seismically triggered landslide dam in Honshiyan, Yunnan, China: from emergency management to hydropower potential. Landslides 12(6):1147–1157

Zhou JW, Xu WY, Yang XG, Shi C, Yang ZH (2010) The 28 October 1996 landslide and analysis of the stability of the current Huashiban slope at the Liangjiaren Hydropower Station, Southwest China. Eng Geol 114(1):45–56

Zhou JW, Cui P, Yang XG (2013) Dynamic process analysis for the initiation and movement of the Donghekou landslide-debris flow triggered by the Wenchuan earthquake. J Asian Earth Sci 76:70–84

Zhou JW, Lu PY, Hao MH (2015) Landslides triggered by the 3 August 2014 Ludian earthquake in China: geological properties, geomorphologic characteristics and spatial distribution analysis. Geomat Nat Haz Risk 7(4):1219–1241